

1 Estimating abiotic thresholds for sagebrush condition class in the western U.S.

2 Stephen P. Boyte ^{a*}, Bruce K. Wylie ^b, Yingxin Gu ^{c1}, Donald J. Major ^d

3 ^a Senior Scientist, KBR, Contractor to the U.S. Geological Survey Earth Resources Observation
4 and Science (EROS) Center, Sioux Falls, SD, 57198, USA

5 ^b Research Physical Scientist, U.S. Geological Survey EROS Center, Sioux Falls, SD 57198,
6 USA

7 ^c Scientist, InuTeq, Contractor to U.S. Geological Survey EROS Center, Sioux Falls, SD, 57198,
8 USA

9 ^d Fire and Landscape Ecologist, Bureau of Land Management, Boise, ID 83709, USA

10 Any use of trade, firm, or product names is for descriptive purposes only and does not imply
11 endorsement by the U.S. Government.

12 *Correspondence: Stephen P. Boyte, USGS, 47914 252nd St, Sioux Falls, SD 57198, USA Tel.:
13 +1 605 594 6171. E-mail address: sboyte@contractor.usgs.gov (S.P. Boyte).

14 ¹Present address: I.M. Systems Group, Inc., at NOAA NESDIS Center for Satellite Applications
15 and Research, College Park, MD 20740, USA

16

17

18

19

20

21 **Abstract**

22 Sagebrush ecosystems of the western U.S. can transition from extended periods of
23 relatively stable conditions to rapid ecological change if acute disturbances occur. Areas
24 dominated by native sagebrush can transition from species-rich native systems to altered states
25 where non-native annual grasses dominate, if resistance to annual grasses is low. The non-native
26 annual grasses provide relatively little value to wildlife, livestock, and humans and function as
27 fuel that increases fire frequency. The more land area covered by annual grasses, the higher the
28 potential for fire, thus reducing the potential for native vegetation to reestablish, even when
29 applying restoration treatments. Mapping areas of stability and areas of change using machine-
30 learning algorithms allows both the identification of dominant abiotic variables that drive
31 ecosystem dynamics and the variables' important thresholds. We develop a decision-tree model
32 with rulesets that estimate three classes of sagebrush condition [i.e. sagebrush recovery, tipping
33 point (ecosystem degradation), and stable]. We find rulesets that primarily drive development of
34 the sagebrush recovery class indicate areas of mid elevations (1 602 m), warm 30-yr July
35 temperature maximums (tmax) (30.62 °C), and 30-yr March precipitation averages equal to
36 26.26 mm, about 10% of the 30-yr annual precipitation values. Tipping point and stable classes
37 occur at elevations that are lower (1 505 m) and higher (1 939 m), respectively, more mesic
38 during March and annually, and experience lower 30-yr July tmax averages. These defined
39 variable averages can be used to understand current dynamics of sagebrush condition and to
40 predict where future transitions may occur under novel conditions.

41 **Keywords:** climate, decision-tree model, machine learning, non-native annual grass, sagebrush,
42 western U.S.

43

44

45 **Introduction**

46 Sagebrush (*Artemisia* spp.) ecosystems of the western U.S. are imperiled (Chambers and
47 Wisdom 2009; U.S. Fish and Wildlife Service 2013). Threats to the ecosystems include wildfire,
48 climate change, development, invasion of non-native annual grasses, and expansion of conifers
49 (Chambers et al. 2017). The threats compromise the ecosystems' abilities to provide services like
50 clean water and air, wildlife habitat, forage for grazing, recreational opportunities, and
51 biodiversity (Rose et al. 2015). The amount of area sagebrush currently occupies is little more
52 than half its historical range (Chambers et al. 2017; Davies and Bates 2019). Euro-American
53 migration into the western U.S., and the accompanying increase in disturbances and invasion of
54 non-native grasses, coincided with sagebrush range reduction (U.S. Fish and Wildlife Service
55 2013; Chambers et al. 2017). Disturbances (e.g. land-use change, fire, overgrazing), often
56 multiple compounding disturbances, caused sagebrush ecosystems to transition from extended
57 periods of relatively stable conditions where native shrub and perennial grass species dominated
58 to ecologically degraded conditions where non-native annual grasses invaded and now dominate.
59 To identify transitional locations, we defined criteria for three classes of sagebrush condition,
60 developed a dataset that reflected the classes, integrated the dataset with relevant independent
61 variables into a decision-tree model, and used the resulting model algorithms to develop spatially
62 explicit maps of sagebrush condition class. For purposes of this study, we named the three
63 classes sagebrush recovery, tipping point (representing ecological degradation), and stable.

64 Most restoration efforts in sagebrush ecosystems have been minimally effective
65 (Blomberg et al. 2012; Svejcar et al. 2017). Therefore, recovery to a sagebrush-dominated
66 system after a disturbance can be expensive and take many years, if recovery ever occurs
67 (Svejcar et al. 2017), although recent studies have preliminarily shown enhanced success of

68 sagebrush restoration (Davies et al. 2018; Germino et al. 2018; Davies and Bates 2019).
69 Sagebrush ecosystems vary in their abilities to resist non-native annual grass invasion and
70 recover from disturbance. Systems with low resistance and resilience were manifested in large
71 geographical areas of non-native annual grass stands that have increased fire frequencies and
72 threaten adjacent healthy rangeland systems. Chambers et al. (2007) found that specific factors
73 influenced how vulnerable a sagebrush ecosystem was to cheatgrass (*Bromus tectorum* L)
74 invasion, the most ubiquitous non-native annual grass in the study area. Climate, disturbance
75 regime, the competitive abilities of the resident species, and traits of the invader were all
76 influential factors of invasibility. Invasibility increased when resources were unused by native
77 vegetation, such as after a fire (Rau et al. 2014; Roundy et al. 2018). Invasion also occurred
78 when resource availability was inconsistent (Rau et al. 2014), which led to periods when
79 resource supply exceeded the resident species' ability to utilize it while invasive species'
80 propagule pressure existed (Davis et al. 2000). This phenomenon could have occurred in low to
81 mid elevations of the sagebrush steppe (Chambers et al. 2014) where precipitation exhibited high
82 temporal variability (Bradley and Mustard 2005). In areas of relatively high perennial vegetation
83 productivity, greater resource utilization by perennial vegetation reduced ecosystems'
84 invasibility (Chambers et al. 2014). How efficient an invading plant was at using resources when
85 they become available could have determined a plant's invasion success (Bansal et al. 2014).
86 Greater resilience levels have been positively associated with higher precipitation, greater soil
87 resources, and higher plant productivity, and linked to higher levels of resistance (Chambers et
88 al. 2014).

89 The goals of this study were to identify abiotic variables that most influenced the
90 prediction of three classes of sagebrush condition and to establish the most common

91 environmental thresholds that characterized each class. We clarified and defined some of the
92 abiotic characteristics and associated thresholds that influenced sagebrush ecosystems' resilience
93 to disturbance, invasibility to non-native annual grasses, and stability. We parameterized
94 decision-tree software in two ways so that it generated 1) a predictive model based on a tree
95 structure and 2) a descriptive model based on rulesets. These two models allowed us to achieve
96 the following objectives:

- 97 1) Develop a spatially explicit predictive map of three classes of sagebrush condition.
- 98 2) Develop a spatially explicit ruleset map that shows where every ruleset occurred.
- 99 3) Identify abiotic variables that most strongly drive development of the sagebrush
100 condition class model.
- 101 4) Establish thresholds of the most commonly used abiotic variables that delineate each
102 sagebrush class.

103 **Methods**

104 *Study area*

105 We focused our study on arid and semiarid sagebrush ecosystems in the western U.S.
106 where annual grass invasion was likely, sagebrush was native, and wildlife and livestock graze.
107 The study excluded areas higher than 2 250 m elevation because cheatgrass was much less likely
108 to invade at elevations above about 2 000 m in the northern Great Basin (Boyte et al. 2015) and
109 because these areas were more resistant to cheatgrass invasion and more resilient to disturbances
110 than areas at lower elevations (Chambers et al. 2014). Also excluded were areas where the 2011
111 National Land Cover Database (The National Land Cover Database 2011) classified a pixel as
112 something other than shrub or herbaceous/grassland (Fig. 1). Excluded areas were masked and
113 neither mapped nor included in processes and analyses.

114 The study area encompassed 286,574 km² including parts of 6 states. The 30-yr (1981 –
115 2010) climate averaged equal 337 mm of precipitation, a minimum temperature of 0° C, and a
116 maximum temperature of 14° C (PRISM Climate Group). The elevation minimum equaled 568
117 m with a mean of 1 562 m when the 2 250 m limit was observed (North American Vertical
118 Datum 88). The topography varied substantially with alternating mountains and valleys
119 throughout much of the study area. The vegetation was composed of mostly shrubs, native
120 grasses, and invasive grasses with the dominant shrubs being sagebrush (*Artemisia* spp.). Some
121 of the common sagebrush species included Basin big sagebrush (*A. tridentata* Nutt. *ssp.*
122 *tridentata*), Wyoming big sagebrush (*A.t.* Nutt. *ssp. wyomingensis* Beetle & Young), and low
123 sagebrush (*A. arbuscula* Nutt.) Other common shrub species included shadscale saltbush
124 (*Atriplex confertifolia* [Torr. & Frem.] S. Watson), rabbitbrush (*Chrysothamnus* spp.),
125 greasewood (*Sarcobatus* spp. Nees), and some antelope bitterbrush (*Purshia tridentata* [Pursh]
126 DC.). Grasses included Sandberg bluegrass (*Poa secunda*), basin wildrye (*Leymus cinereus*
127 [Scribn. & Merr.] Á. Löve), Idaho fescue (*Fescue idahoensis* Elmer), and the introduced crested
128 wheatgrass (*Agropyron cristatum* L.). Several annual grasses have invaded the study area
129 including cheatgrass, North African wire grass (*Ventenata dubia* [Leers] Coss.), medusahead
130 (*Taniatherum* spp.), and, in the warmest and most arid places, red brome (*Bromus rubens* L.).

131 *Datasets*

132 We categorized the datasets used in this study into two types: 1) the sagebrush condition
133 class reference dataset. This dataset was developed from four remotely sensed derived datasets,
134 and parameters were defined by the sagebrush condition criteria. The four datasets were
135 described in the next four subsections, and the sagebrush condition criteria were defined in the
136 subsection “Sagebrush Condition Classes”; and 2) datasets used as drivers in the decision-tree

137 model. The model drivers included an elevation dataset that was derived from The National Map
138 (<https://nationalmap.gov/elevation.html>). The elevation dataset had a native 30-m spatial
139 resolution, and we spatially averaged it using a 7x7 focal scan and resampled it to 250 m using
140 nearest neighbor. Polaris soils data were 78-m native spatial resolution data. We spatially
141 averaged those data using a 3x3 focal scan, and then resampled them to 250 m using nearest
142 neighbor. The climate data, which included 30-yr annual, seasonal, and monthly precipitation
143 and temperature minimums and maximums (PRISM Climate Group), were resampled from 800
144 m to 250 m using bilinear interpolation.

145 The four remotely sensed derived datasets described next used Moderate Resolution
146 Imaging Spectroradiometer (MODIS) sensor's Normalized Difference Vegetation Index (NDVI)
147 data (Jenkerson et al. 2010) at 250-m spatial resolution. NDVI allows the monitoring of seasonal
148 and interannual vegetation greenness and has been used to measure green biomass (Jensen 2005).
149 We applied regression-tree optimization protocol (Gu et al. 2016; Wylie et al. 2018) to the
150 development of all regression-tree models to minimize each models' errors and overfitting
151 tendencies.

152 *Annual herbaceous percent cover*

153 We developed and published a time series (2000 – 2016) of spatially explicit annual
154 herbaceous percent cover estimates (Boyte and Wylie 2017) at 250-m spatial resolution
155 throughout much of the western U.S. While the time series estimated annual herbaceous percent
156 cover, the primary annual herbaceous type targeted was cheatgrass because of its pervasive
157 dominance in sagebrush ecosystems. Cheatgrass was highly responsive to annual precipitation
158 (Bradley and Mustard 2005; Pilliod et al. 2017), leading to temporal variation in annual
159 herbaceous percent cover. Annual herbaceous percent cover demonstrated high spatial variation

160 because of biophysical factors and a history of disturbances (Chambers et al. 2014). We
161 developed the annual herbaceous estimates using a regression-tree model integrated with field-
162 based, remotely sensed, climate, fire, and biophysical data (Boyte et al. 2019a). The model used
163 more than 30,000 field-based training data points from 5 years (Boyte et al. 2019a) to develop
164 spatially explicit estimates of annual herbaceous percent cover (see Table 1 for model accuracy
165 assessments). We used 17 years of 7-day pixel composites of NDVI data to map the wide-
166 ranging annual herbaceous percent cover dynamics inherent to the water-limited sagebrush
167 ecosystem. Driving variables for the model included native 250-m remotely sensed derivatives –
168 annual growing season NDVI, summer NDVI, and start of season time (a phenology measure).
169 Additional variables consisted of a year-since-fire dataset, PRISM 30-yr precipitation (PRISM
170 Climate Group), Polaris soils data – organic matter and available water capacity, and topographic
171 data – elevation, a wetness index, and north- and south-facing slope indices. Aspects were
172 defined by azimuths between 315° and 45° (north aspects) and 135° and 225° (south aspects) on
173 slopes greater than 8.5% (where aspect angles were measured in a clockwise direction and north
174 = 0°). Undefined aspects were assigned a null value.

175 *Sagebrush percent cover*

176 Aggregated 250-m enhanced MODIS NDVI from weeks 15 – 40 of each year of the
177 study period (2001 – 2015) served as the growing season NDVI. Sagebrush percent cover was a
178 derivative of growing season NDVI, calculated on a pixel-by-pixel basis using the following
179 algorithm (Eq. 1) (Rigge et al. 2019).

$$180 [(0.4247 * \textit{Annual growing season NDVI}) - 43.839] \quad [1]$$

181

182 *Sagebrush Ecosystem Performance Anomaly*

183 In sagebrush ecosystems, annual grasses influenced the NDVI signal, which could have
184 caused sagebrush percent cover to be overestimated, especially in recently disturbed areas. To
185 mitigate this problem, we developed a regression-tree model that predicted sagebrush percent
186 cover by incorporating seasonal and monthly weather data to separate effects of disturbances and
187 land management from effects of weather (Wylie et al. 2012). The dataset was the sagebrush
188 ecosystem performance anomaly, or sagebrush anomaly, and it introduced temporal variation
189 throughout the study period.

190 We calculated the difference between the sagebrush percent cover and the predicted
191 sagebrush percent cover datasets and used statistical confidence levels to define normal and
192 abnormal ecosystem performance on an annual time step (Wylie et al. 2008; Gu and Wylie 2010;
193 Wylie et al. 2012; Rigge et al. 2013). We labeled pixels of abnormal performance as
194 overperformance and underperformance depending on whether a pixel fell above or below the
195 95% confidence level, respectively. Pixels with high normal or overperformance that also
196 experienced high levels of annual grass percent cover ($\geq 10\%$) and low levels of tree cover (\leq
197 15%) were pixels of likely sagebrush overestimation and not included as reference data.

198 *Sagebrush site potential*

199 Sagebrush site potential was developed as a measure of an ecosystem's inherent
200 productivity (Wylie et al. 2008) and, in this study, represented the long-term average production
201 of sagebrush biomass in a good sagebrush state, i.e. non-degraded or non-disturbed (Rigge et al.
202 2019). Site potential introduced spatial variability across the study area, whereas the sagebrush
203 anomaly, sagebrush percent cover, and annual herbaceous percent cover datasets introduced
204 temporal variability throughout the study period. We defined a pixel as in good sagebrush state if

205 more than 40% of a pixel's vegetation cover was sagebrush, less than 10% of its absolute cover
206 was annual herbaceous, and no fires burned in the pixel from 1993 – 2014. A final criterion
207 required that more than 70% of the pixel be classified by the National Land Cover Database as
208 shrub or herbaceous/grassland land cover.

209 Long-term (2000 – 2015), above-average growing season NDVI from MODIS at 250-m
210 resolution served as a proxy for sagebrush site potential. The MODIS NDVI values ranged from
211 -0.01 to 0.59 on a scale of -1 to 1. A random stratification of pixels that met the definition of a
212 good sagebrush state were selected as training samples, with a low sagebrush productivity tier
213 ranging from -0.01 to 0.14 (n = 3 543), a moderate tier ranging from 0.15 to 0.22 (n = 3 695),
214 and a high tier ranging from 0.23 to 0.59 (n = 3 514). Site potential was modeled in regression-
215 tree software, and model accuracy assessments are displayed in Table 1. The model was driven
216 by Polaris soils data – organic matter and available water capacity – at 0 to 30 cm depth, a
217 compound topographic index, steep north- and south-facing slopes, and Landsat-based NDVI.
218 The Landsat-based NDVI was, on a pixel-by-pixel basis, the value equal to the NDVI's 90th
219 percentile in the months of August and September from 1986 – 2013. Landsat NDVI values used
220 in the study were unlikely to be affected by disturbances that occurred after 1986. Landsat NDVI
221 data were native 30-m spatial resolution data that we spatially averaged using a 7x7 focal scan
222 and then resampled to 250 m.

223 *Sagebrush condition classes*

224 We developed criteria that defined three classes of sagebrush condition – sagebrush
225 recovery, tipping point, and stable. The criteria were limited by the study period (2000 – 2015)
226 and determined using the four remotely sensed derived datasets just described. Any pixel that
227 met the criteria for a specific class was a reference data candidate unless the pixel met the criteria

228 for more than one class, then it was removed from the pool of reference data candidates. We
229 classified a pixel as sagebrush recovery if it met two criteria: 1) for at least 3 years early (2001 –
230 2010) in the time series, that pixel had annual grass percent cover $\geq 10\%$, sagebrush site potential
231 $> 7\%$, sagebrush anomaly was high normal performance or above, and tree canopy $\leq 15\%$; and,
232 2) for at least 3 years late (2011 – 2015) in the time series, that same pixel had annual grass
233 percent cover $< 10\%$, sagebrush percent cover $> 10\%$, and sagebrush anomaly was normal, i.e., it
234 functioned as we expected sagebrush should. A total of 61 444 pixels, or 1.3% of unmasked
235 pixels, met the sagebrush recovery criteria. Pixels that met the criteria for a specific class could
236 be randomly selected as a dependent variable in the sagebrush condition class model.

237 We classified a pixel as tipping point if it met two criteria: 1) for 2 years early (2001 –
238 2005) in the time series, the pixel had annual grass percent cover $< 10\%$, sagebrush percent cover
239 $> 7\%$, and normal sagebrush anomaly; and, 2) for at least 2 years late (2011 – 2015) in the time
240 series, that same pixel had annual grass percent cover $\geq 10\%$, sagebrush site potential was at
241 least moderate ($> 7\%$), and sagebrush anomaly was at least high normal – high normal to
242 overperformance sagebrush anomaly can indicate cheatgrass presence. A total of 101 663 pixels,
243 or 2.2% of unmasked pixels, met the tipping point criteria.

244 We classified a pixel as stable if it met two criteria: 1) for 13 or more years during the
245 study period, the pixel had annual grass percent cover $< 10\%$, normal sagebrush performance,
246 and annual grass percent cover no more than one standard deviation from the study period mean
247 for that pixel; and, 2) for 13 or more years during the study period, that same pixel had sagebrush
248 percent cover $> 7\%$ and sagebrush percent cover no more than one standard deviation from the
249 study period mean for that pixel. A total of 11 029 pixels, or 0.24% of unmasked pixels, met the
250 stable criteria.

251 When the decision-tree software classified a pixel using the tree structure, it established a
252 confidence level for that prediction using a value between 0 and 1 (Quinlan 2013). The class
253 confidence levels for the sagebrush class condition model ranged from 0.33 to 1.00. We defined
254 a class confidence level equal to or greater than 0.70 as high probability, a class confidence level
255 equal to or greater than 0.50 and less than 0.70 as moderate probability, and a class confidence
256 level equal to or greater than 0.33 and less than 0.50 as low probability.

257 *Model development*

258 The decision-tree model used, See5 (<https://www.rulequest.com/>), was designed to obtain
259 information from databases of primary (dependent variable) and ancillary (independent
260 variables) data and then construct diagnostic rules based on that information to predict discrete
261 classes (Quinlan 2013). We developed a database with a randomly stratified sample of pixels (n
262 = 16 550), of which 15% met the criteria for stable pixels, 32% for sagebrush recovery pixels,
263 and 53% for tipping point pixels. We used a sample of possible pixels because pixels that met the
264 criteria for the stable class equaled only about 6% of all possible reference data pixels. To avoid
265 underrepresenting the stable class in our model, we set a minimum requirement of 2 500 pixels
266 from each class. To avoid both spatial autocorrelation issues and overrepresenting the tipping
267 point class, we limited the number of sample pixels from that class. We developed a test dataset
268 of 2 500 pixels that was a random subset of all potential dependent variable pixels not used for
269 model training. The test dataset provided an independent validation of model accuracy. We also
270 calculated a ten-fold cross validation of the training data, which provided a second independent
271 validation of model accuracy.

272 We developed two classification models (Fig. 2): one to predict classes and a second to
273 describe rulesets that defined how independent variables were used. The predictive model used a

274 tree structure and ran with no user-defined constraints to its number of nodes, allowing the
275 modeling software to use an automated protocol to prune the tree. A mapping software,
276 MapSee5, applied the See5 classifiers to the independent variables' imagery to generate a
277 sagebrush condition class prediction map (Boyte et al 2019b) . The descriptive model utilized a
278 user-defined number of rulesets. Limiting the number of rulesets greatly enhanced the user's
279 ability to interpret the associated thresholds of independent variables but sacrificed some
280 accuracy. A low number of rulesets facilitated the ecological interpretation of the rulesets, which
281 increased the understanding of the descriptive model (Quinlan 2013). We included identical
282 drivers for both models, and they were 30-yr climate, elevation, and soils data. The 30-yr climate
283 data included average annual values, average values of selected months, and average seasonal
284 values for spring (March – May) and summer (June – August). Precipitation (ppt), temperature
285 maximums (tmax), and temperature minimums (tmin) were the 30-yr climate variables used. The
286 soils data included Polaris soil organic matter and available water capacity (Table 2). Of the 30
287 variables integrated into the sagebrush condition models, 6 were identified as being most
288 impactful to the development of both the predictive and the descriptive models. These six
289 variables were analyzed and used to delineate thresholds that characterized sagebrush condition.

290 We also analyzed the output of the descriptive model that defined the rulesets, identified
291 confidence levels for rulesets and their associated classes, and calculated the geographical space
292 each ruleset covered. The rulesets were input into a conditional-statement model that mapped
293 each ruleset in its spatial context based on stratification thresholds from the independent
294 variables (Fig. 3). The descriptive model incorporated 21 rules using 15 independent variables.
295 Nine rulesets defined the variable conditions that made up the tipping point class, and the ruleset
296 from that class with the highest prediction confidence (0.839) is shown below. This ruleset

297 constituted about 2.39% of all training points, 1 390 km² of the study area, and defined a tipping
298 point as:

299 Elevation >1602 m AND ≤1798 m

300 April ppt > 19 mm

301 Summer ppt ≤ 26 mm

302 June tmin ≤ 26 °C

303 Summer tmin ≤35 °C.

304

305 *Validation*

306 We validated the sagebrush condition class map using two datasets and methods. First,
307 we acquired from Bureau of Land Management (BLM) staff 2013 – 2016 BLM Assessment
308 Inventory and Monitoring (AIM) plot-level data that were collected from the field, typically
309 using the line-point intercept method at three transects of 30 m each within a spoke design
310 (Herrick et al. 2017). Field data that can be used to validate remotely sensed data were difficult
311 and expensive to gather and process and were therefore relatively scarce (Browning et al. 2015;
312 Bradley et al. 2018). Field data that matched the spatial resolution of a 250-m eMODIS NDVI
313 pixel were even more uncommon. Once obtained, field data can be hard to apply to remotely
314 sensed data (Bradley et al. 2018), especially remotely sensed data with coarser spatial
315 resolutions. The AIM data were ubiquitous for our study area and period, and for our purposes,
316 provided an acceptable measure of validation.

317 We examined the AIM plot-level data for percent cover of sagebrush and non-native
318 annual grasses and compared those data to corresponding pixels and their predicted classes. If
319 the sagebrush and invasive annual grass percent cover values for an AIM plot matched a specific
320 class' criteria, and that class corresponded to the class represented on the predictive map, then
321 that data point was considered correct. If the non-native annual grass percent cover for any AIM
322 field plot was equal to or greater than 15%, then the pixel had to be classified as tipping point to

323 be correct, regardless of the percent cover of sagebrush because areas with this level of
324 cheatgrass were more likely to have burned (Bradley et al. 2018) and therefore, for this study's
325 purpose, were identified as a tipping point. Finally, if sagebrush and invasive annual grass
326 percent cover values of a plot did not meet the criteria for any class, then the data point was
327 removed from the analysis because the data point may have been associated with factors other
328 than those that defined the sagebrush condition classes.

329 Second, we overlaid Monitoring Trends in Burn Severity (MTBS) polygons from 2001 –
330 2015 on the sagebrush condition class map (Monitoring Trends in Burn Severity 2018). MTBS
331 polygons in the western United States represented wildland fires in almost all circumstances
332 because of the relative infrequency of prescribed fires in the West and the minimum 1 000-acre
333 fire-size threshold used to establish the polygon extents (Joshua Picotte, Fire Specialist, MTBS
334 Science Support, written communication, 25 September 2019). We calculated the percent of total
335 area burned by class for each year. While we display all study period years in Figure 4, we focus
336 the validation on the last 5 years of the study period because of the time dimension used in our
337 criteria to define classes. This time dimension focused the transition from a tipping point to a
338 sagebrush recovery class and the transition from a stable sagebrush ecosystem state to a tipping
339 point class on the last 5 years of the time series. Given this time dimension, the last 5 years of the
340 time series were most critical in assessing the accuracy of these datasets. The MTBS polygons
341 were used to help define sagebrush site potential, but the effect on the sagebrush condition
342 classes would likely be relatively minimal as only two of its criteria used site potential in their
343 definitions.

344

345

346 **Results**

347 *Model development*

348 The predictive and descriptive models used independent variables to drive model
349 development, and although the same variables were available to both models, the predictive
350 model used all available variables whereas the descriptive model used only some (Table 2). The
351 two models also used variables at different frequencies. These phenomena primarily occurred
352 because we developed the predictive model by applying few constraints to the decision trees that
353 predicted classes, and we developed the descriptive model by severely limiting the number of
354 rulesets that described how independent variables were associated with each class.

355 Model variable usage was presented as a percentage and calculated by the decision-tree
356 software based on if the value of the variable was known and if the variable was used in the
357 prediction of a class (Quinlan 2013). Multiple variables' model usage frequencies equal 100% in
358 the predictive model, including elevation and 30-yr precipitation. These two variables were most
359 frequently used in the descriptive model at 75% and 73%, respectively. The frequent use of these
360 variables in both models indicated their heavy influence in classifying sagebrush condition.
361 Other variables of importance for both the predictive and the descriptive models were available
362 water capacity, 30-yr July temperature maximum, and 30-yr March temperature minimum. July
363 weather variables, collectively, influenced the predictive model more than any other month's
364 weather variables, although March weather variables were almost as influential. March and July
365 weather variables were the weather variables used most frequently in the descriptive model,
366 although their frequency of use was much less than in the predictive model and much less than
367 elevation and 30-yr precipitation. May was the month with weather variables least used in the
368 predictive model. Seasonal and other monthly weather averages were relatively influential in the
369 predictive model, but many were used sparingly or not at all in the descriptive model. Summer

370 temperature maximum was not used in the descriptive model and was used the least in the
371 predictive model, indicating little influence on sagebrush condition class.

372 *General characteristics of dominant variables*

373 To establish the general characteristics of the dominant variables associated with each
374 class – sagebrush recovery, tipping point, stable – we calculated a weighted average based on the
375 percentage of study area covered by each ruleset and connected the averages to the most
376 frequently used variables in the descriptive model (Table 3). We also analyzed the dominant
377 variable thresholds defined by the rules in the descriptive model. Elevation and 30-yr average
378 precipitation overwhelmingly drove model development, and distinct differences existed for
379 elevation and 30-yr precipitation averages between sagebrush condition classes. The stable class
380 was substantially more mesic and at higher elevations than either the sagebrush recovery or
381 tipping point classes. Data also indicated that the stable class was cooler during March and July.
382 The sagebrush recovery class occurred at elevations slightly higher than the tipping point class,
383 but the tipping point class was more mesic, and, during mid-summer, cooler. The values for
384 available water capacity varied little between classes, but soil organic matter increased from
385 sagebrush recovery (38.85 kg • m⁻²) to tipping point (79.92 kg • m⁻²) to stable (108.10 kg • m⁻²)
386 classes. The tipping point class covered a substantial majority of the study area, so we expected,
387 on average, this class to be the most variable.

388 *Characteristic thresholds of dominant variables*

389 Table 4 shows the variables that were the most impactful drivers for both the predictive
390 and descriptive models and connects those drivers to the rulesets they influenced. Less
391 commonly used drivers did influence the rulesets, but there were too many (30) to display

392 concisely and cogently, and their impact on the development of the descriptive model was
393 relatively minimal. Several elevation values served as thresholds to develop the descriptive
394 model, but one value, 1 602 m, was present in 71% of all rulesets, including 6 of the 7 rulesets
395 for the sagebrush recovery class. The tipping point class used the 1 602 m elevation threshold in
396 6 of its 9 rulesets, and for this class, at least 35% of the overall study area was defined by rulesets
397 at or below 1 602 m with 22% at or below 1 339 m elevation. Less than 4% of the study area in
398 this class was defined by rulesets higher than 1 602 m. All rulesets in the stable class were
399 defined by elevations above 1 602 m with 3 of its 5 rulesets defined by > 1 602 m threshold. The
400 weighted average elevation for the stable class was more than 338 m higher than either of the
401 other two classes. The 30-yr precipitation variable threshold that predominated in the descriptive
402 model's development was 338 mm, a number almost identical to the overall study area's 30-yr
403 precipitation average (337 mm). This threshold value was present in 48% of all rulesets
404 including all five of the stable class' rulesets, a class that was mostly present at higher elevations.
405 Rulesets 14 (tipping point class) and 18 (stable class) showed 30-yr precipitation threshold
406 values at > 338 mm, and these two rulesets' average elevations were 1760 m and 2129 m,
407 respectively, substantially higher than their class means. Generally, rulesets that primarily drove
408 development of the sagebrush recovery class indicated areas of mid elevations, warm July
409 temperature maximums, and 30-yr March precipitation averages about 10% of the 30-yr average
410 precipitation values. For the tipping point class, rulesets occurred at the lowest average
411 elevations of the three classes, although the elevation range was widest. Annual precipitation
412 totals were about halfway in between the other two classes, and March temperature minimums
413 were lower than freezing (0 °C). Variables that drive development of the stable class indicated
414 space that was at considerably higher elevations, received substantially more average annual

415 precipitation, and had considerably lower average March temperature minimums than the other
416 two classes.

417 *Spatial representation of the descriptive model*

418 Figure 3 displays the spatial arrangement of the rulesets defined by the descriptive model.
419 Multiple rulesets can apply to an individual pixel, but we programmed the conditional-statement
420 model so that a ruleset with the highest accuracy spatially defined a pixel, superseding rulesets
421 with lower accuracies. The rules from the tipping point class (rulesets 8 – 16) cover 70.36% of
422 the study area including highly populated areas in Idaho’s Snake River Plain where elevations
423 were lower than average, fires were relatively common, and ecosystem transformations were
424 often driven by human activities. Northeastern and north-central Nevada were predominantly
425 covered by the sagebrush recovery class (rulesets 1 – 7; 21.29% of study area), specifically
426 rulesets 1 and 7. The stable class (rulesets 17 – 21; 8.35% of study area) mainly occupied areas
427 of transitional and higher elevations. The average elevation of a stable pixel equaled 1939 m,
428 substantially higher than either of the two other classes (Table 3). Ruleset 1 transitioned into and
429 intermixed with ruleset 10 in north-central and northwest Nevada. Overall, ruleset 1 territory
430 occupied a weighted-average elevation of 1442 m, whereas rule 10 occupied a weighted-average
431 elevation of 1168 m and dominated the low elevation extents of the study area. In the geographic
432 area of northwest Nevada where a basin and range topography of alternating elevations exists,
433 rulesets transitioned relatively frequently with elevation changes. The sagebrush recovery and
434 stable classes encompassed much of the northwesternmost corner of Nevada, coinciding with
435 higher elevations. The stable class occupied the highest elevations in this geographic area and in
436 northeast Nevada and in the northeast corner of the study area. With few exceptions,
437 southeastern Oregon was covered by tipping points rules and mostly occupied low and relatively

438 low elevations. The 30-yr annual precipitation averaged in this area experienced substantial
439 variability with values ranging from 274 mm to 474 mm.

440 *Spatial representation of the predictive model*

441 The predictive model's spatial output (Fig. 5) displayed similar spatial patterns to the
442 descriptive model's patterns of sagebrush recovery, tipping points, and stable classes.
443 Differences exist between the two maps because, as discussed above, the two models were
444 developed with different goals. One area where the two maps deviate was in Idaho on the eastern
445 edge of the Snake River Plain and near the Oregon/Idaho border on the western edge of the
446 Snake River Plain where the predictive model displays sagebrush recovery and the descriptive
447 model displays tipping points. Sagebrush recovery pixels constituted 28.77% of all unmasked
448 pixels, and they were located primarily in north-central and northeast Nevada with some
449 scattered in and around the periphery of the Snake River Plain. Small pockets of recovery existed
450 in topographically diverse areas just west of the Snake River Plain in southeast Oregon. A
451 considerable section of the rest of southeast Oregon was modeled as sagebrush recovery. The
452 majority (57.36%) of the predictive map was classified as tipping point, while much of the
453 northern tier met the classification of high probability. A relatively sizeable section of the study
454 area along the California / Nevada border was also classified as high probability of tipping point.
455 The stable class covered 13.87% of the study area, mostly at higher elevations stretching along
456 and across Nevada's northern border. In the northeast corner of the study area, the stable class
457 frequently intermixed with both sagebrush recovery and tipping point classes.

458

459

460 *Validation*

461 Despite the spatial incongruence between the 250-m datasets used in this study and the
462 AIM data (Boyte et al. 2019a), the overall agreement between the three classes and the field-
463 based AIM data was relatively strong (64.09%) (Table 5). Each year experienced similar overall
464 accuracy, ranging from 62.37% in 2013 to 68.54% in 2014. Accuracies deviated considerably
465 when analyzed based on class. The tipping point class' overall accuracy equaled 73.16% with its
466 highest accuracy during 2015 at 83.26%. This class covered most of the study area. These
467 numbers were much higher than the sagebrush recovery class, which had an overall accuracy of
468 37.84% and a high in 2013 of 44.16%. The stable class performed much like the tipping point
469 class with an overall accuracy of 65.12% and a high in 2013 of 73.91%.

470 When the MTBS polygons were overlaid on the predictive map and compared to the
471 sagebrush condition class underneath, we expected that more of the tipping point class would be
472 encompassed than the other two classes because, by definition, it had a higher percent of highly
473 flammable annual grass cover. Figure 4 showed exactly that phenomenon throughout the time
474 series with more of the burned area occurring in the tipping point class each year. At two points
475 in the time series, 2005 and 2010, the area burned in the tipping point and the sage recovery
476 classes were almost equal. After both of those years, the amount of area burned in the tipping
477 point class increased when compared to the amount of area burned in the sagebrush recovery
478 class. A consistent downward trend appeared from 2011 – 2014 when the sagebrush recovery
479 class declined as a percentage of the total area burned and the tipping point class area
480 encompassed almost 100% of the burned area. There was a slight upturn in burned area for the
481 sagebrush recovery class in 2015. The inverse of that trend occurred in the tipping point class as
482 it increased as a percentage of the total burned area until 2015 when it turned slightly downward.

483 The stable class experienced a consistent downward trend from 2007 until 2012 when a slight
484 increase occurred. The trend for the stable class was downward during the last three years with
485 less than 1.5% of the area burned in that class during both 2014 and 2015.

486 In the last 5 years of the study period, 71.08% of the area that burned was in the tipping
487 point class, 22.50% was in the sage recovery class, and 6.42% in the stable class. In the last 3
488 years of the study period, 91% of burns occurred in the tipping point class. The 5-year burned-
489 area percentages were similar to total-area percentages for the associated classes: tipping point
490 class (70.36%); sage recovery class (21.31%); and stable class (8.35%).

491 **Discussion**

492 Mapping areas of stability and areas of change using machine-learning algorithms
493 allowed both the identification of dominant abiotic variables that drive ecosystem dynamics and
494 the variables' important thresholds. Both the predictive and descriptive models for this study
495 were developed using multiple drivers that represented climatic, topographic, and soils data
496 because these variables were considered among the most important drivers of invasibility of
497 sagebrush ecosystems (Roundy et al. 2018). Resilience to disturbance and stress was associated
498 with climatic and topographic gradients, resistance to cheatgrass invasion was driven by
499 temperature and precipitation regimes (Chambers et al. 2014), and the driver of variable
500 interannual cheatgrass growth was highly variable precipitation (Bradley and Mustard 2005).
501 Periods of limited soil moisture reduced plant germination and establishment (Bishop et al.
502 2019), and management activities that sought to exclude non-native species introduced gaps in
503 vegetation cover that caused increases in resource availability (Rau et al. 2014). Both phenomena
504 created space for cheatgrass, an early-season and fast-growing plant, to have invaded by

505 capitalizing on available moisture and nutrients when temperatures warmed, earlier than most
506 native plants (Boyte et al. 2016).

507 Elevation was the most often-used variable in development of both the predictive and
508 descriptive models, and the 1 602 m elevation threshold played an important role in ruleset
509 development of the descriptive model. This elevation threshold was slightly above the mean
510 elevation (1 562 m) for the overall study area, and substantially above the low end of the
511 elevation range of 568 m. Elevation affected sagebrush invasibility indirectly through air and soil
512 temperatures, plant communities and types, and plant productivity (Chambers et al. 2014).
513 Historically, fire events were more common at higher elevations in the Great Basin than at lower
514 elevations because higher plant productivity led to more continuous fuels that spread fire, and
515 plants adapted to fire as a result (Chambers et al. 2014). The lower native plant productivity at
516 lower, drier elevations left adequate space for annual grasses to invade and exploit unused
517 resources.

518 The elevational influence was evident in the study as 50% of the area classified as tipping
519 point was defined by elevation thresholds lower than 1 602 m with almost 33% being lower than
520 1 339 m. Less than 4% of the tipping point class' area had an elevation threshold above 1 602 m.
521 Better soil productivity at higher elevations increased plant productivity, which increased
522 resistance to annual grass invasion, and while available water capacity varied little among
523 sagebrush condition classes, soil organic matter was positively correlated with elevation. While
524 we did not show both resiliency and resistance in the same pixel, we can presume that the stable
525 class was derived from a pixel's resistance to invasion, which was positively associated with
526 resilience to disturbance (Chambers et al. 2014). The stable class was defined much differently
527 than the other two classes when weighted averages of the most important variables were

528 considered (Table 3). The stable class was substantially more mesic and much cooler, typical of
529 higher elevation sites in the study area.

530 The 30-yr precipitation variable was used nearly as often as elevation in development of
531 the predictive and descriptive models, demonstrating its strong influence on sagebrush condition
532 class. The area mapped as tipping point class had higher average precipitation than the sagebrush
533 recovery class, which seemed counter intuitive. However, given that the tipping point class
534 covered more than 70% of the study area and with the wide diversity of sagebrush and annual
535 grass productivity, these large-area precipitation (and elevation) means included a fair amount of
536 site-specific variability. In addition, both elevation and precipitation played important roles in the
537 separation of recovery versus tipping point areas, so the combined stratification of the
538 classification-tree structure in precipitation and elevation may well account for much of the sub-
539 regional deviations from these large and diverse area precipitation means.

540 In the northern Great Basin, March temperatures, much more than March precipitation,
541 proved influential in a study that modeled and analyzed cheatgrass percent cover predictions
542 using current and future climate data (Boyte et al. 2016). In the current study, March
543 precipitation was one of the strongest drivers of sagebrush condition class while March
544 temperature variables still exerted substantial influence on both the predictive and descriptive
545 models. March's climate was important to cheatgrass's life cycle and its ability to compete with
546 native plants in the semiarid Great Basin (Roundy et al. 2018), and with a weighted 30-yr
547 average March temperature minimum below freezing for all classes (-5.38 °C for the stable
548 class) (Table 3), cheatgrasses' ability to survive drops in temperatures below 0 °C (Bykova and
549 Sage 2012) was observed. Annual average precipitation was identified by Bradley (2009) as a
550 strong predictor of cheatgrass presence in the Great Basin, and this variable was strongly

551 influential to the development of both the predictive and descriptive models. As a dominant
552 driver of thresholds, 30-yr annual precipitation influenced 48% of the rulesets that covered 43%
553 of the study area.

554

555 **Implications**

556 The spatially explicit maps revealed that most of the study area has been altered from its
557 native state and has never recovered. These tipping points are likely to persist in the future as
558 natural recovery in sagebrush ecosystems is a long-term process and restoration efforts can be
559 marginally effective. Oftentimes subsequent disturbances interrupt natural recovery and
560 restoration projects. Some areas have recovered or have been restored as evidenced by sagebrush
561 recovery pixels. Stable pixels existed where sagebrush systems are most likely to persist in the
562 future, although climate change can threaten the persistence of stable areas. The predictive model
563 can be modified with future climate data to aid in identifying future achievable sagebrush
564 recovery or stable persistence.

565 The study delineated the abiotic variables that most influence the development of the
566 sagebrush condition models. The descriptive model is unique in that it provides relative values
567 that define the most influential variable's thresholds. The values give clarity to some of the
568 forces that drive sagebrush ecosystem stability and change. The study's findings have
569 implications for land managers, ecologists, fire modelers, and policymakers as they identify
570 potential areas of disturbance, recovery, and stability and determine the best way forward to
571 preserve sagebrush ecosystems and the species that inhabit them. Given the scale of the study
572 area and the adequate geographic distribution of sampling points, analyzing relationships among

573 these forces and ecosystem change can elicit a better understanding of sagebrush ecosystems and
574 enhance land management and policymaking efforts.

575 **Acknowledgements**

576 We thank Neal Pastick for his astute insights on the modeling process and his input to an earlier
577 version of the manuscript. U.S. Geological Survey Land Change Science and National Land
578 Imaging programs and the Bureau of Land Management funded the study. The funders had no
579 role in the study or preparation of this manuscript.

580 **References**

- 581 [dataset] Boyte, S.P., Wylie, B., Gu, Y., 2019b. Estimating environmental thresholds for three classes of
582 sagebrush condition in the western United States (2001 – 2015). U.S. Geological Survey data release.
583 <https://doi.org/10.5066/P98WBAL4>.
- 584 [dataset] Boyte, S.P., Wylie, B.K., 2017. A time series of herbaceous annual cover in the sagebrush
585 ecosystem. U.S. Geological Survey data release. <https://doi.org/10.5066/F71J98QK>.
- 586 Bansal, S., James, J.J., Sheley, R.L., 2014. The effects of precipitation and soil type on three invasive
587 annual grasses in the western United States. *J Arid Environ.* 104, 38-42.
588 <http://dx.doi.org/10.1016/j.jaridenv.2014.01.010>.
- 589 Bishop, T.B.B., Munson, S., Gill, R.A., Belnap, J., Petersen, S.L., St Clair, S.B., 2019. Spatiotemporal
590 patterns of cheatgrass invasion in Colorado Plateau National Parks. *Landsc Ecol.* 34, 925-941.
591 <https://doi.org/10.1007/s10980-019-00817-8>.
- 592 Blomberg, E.J., Sedinger, J.S., Atamian, M.T., Nonne, D.V., 2012. Characteristics of climate and landscape
593 disturbance influence the dynamics of greater sage-grouse populations. *Ecosphere.* 3, 1-20.
594 [10.1890/ES11-00304.1](https://doi.org/10.1890/ES11-00304.1).
- 595 Boyte, S.P., Wylie, B.K., Major, D.J., 2016. Cheatgrass Percent Cover Change: Comparing Recent
596 Estimates to Climate Change - Driven Predictions in the Northern Great Basin. *Rangeland Ecol Manag.*
597 69, 265-279. <http://dx.doi.org/10.1016/j.rama.2016.03.002>.
- 598 Boyte, S.P., Wylie, B.K., Major, D.J., 2019a. Validating a Time Series of Annual Grass Percent Cover in the
599 Sagebrush Ecosystem. *Rangeland Ecol Manag.* 72, 347-359. <https://doi.org/10.1016/j.rama.2018.09.004>.
- 600 Boyte, S.P., Wylie, B.K., Major, D.J., Brown, J.F., 2015. The integration of geophysical and enhanced
601 Moderate Resolution Imaging Spectroradiometer Normalized Difference Vegetation Index data into a
602 rule-based, piecewise regression-tree model to estimate cheatgrass beginning of spring growth. *Int J*
603 *Digit Earth.* 8, 118-132. <https://dx.doi.org/10.1080/17538947.2013.860196>.
- 604 Bradley, B.A., 2009. Regional analysis of the impacts of climate change on cheatgrass invasion shows
605 potential risk and opportunity. *Glob Change Biol.* 15, 196-208. [http://dx.doi.org/10.1111/j.1365-](http://dx.doi.org/10.1111/j.1365-2486.2008.01709.x)
606 [2486.2008.01709.x](http://dx.doi.org/10.1111/j.1365-2486.2008.01709.x).
- 607 Bradley, B.A., Curtis, C.A., Fusco, E.J., Abatzoglou, J.T., Balch, J.K., Dadashi, S., Tuanmu, M.N., 2018.
608 Cheatgrass (*Bromus tectorum*) distribution in the intermountain Western United States and its

609 relationship to fire frequency, seasonality, and ignitions. *Biological Invasions*. 20, 1493-1506.
610 <https://doi.org/10.1007/s10530-017-1641-8>.

611 Bradley, B.A., Mustard, J.F., 2005. Identifying land cover variability distinct from land cover change:
612 Cheatgrass in the Great Basin. *Remote Sens Environ*. 94, 204-213.
613 <https://doi.org/10.1016/j.rse.2004.08.016>.

614 Browning, D.M., Rango, A., Karl, J.W., Laney, C.M., Vivoni, E.R., Tweedie, C.E., 2015. Emerging
615 technologies and cultural shifts advancing drylands research and management. *Frontiers in Ecology and
616 the Environment*. 13, 52-60. <https://doi.org/10.1890/140161>.

617 Bykova, O., Sage, R.F., 2012. Winter cold tolerance and the geographic range separation of *Bromus*
618 *tectorum* and *Bromus rubens*, two severe invasive species in North America. *Glob Chang Biol*. 18, 3654-
619 3663. <https://doi.org/10.1111/gcb.12003>.

620 Chambers, J.C., Bradley, B.A., Brown, C.S., D'Antonio, C., Germino, M.J., Grace, J.B., Hardegree, S.P.,
621 Miller, R.F., Pyke, D.A., 2014. Resilience to stress and disturbance, and resistance to *Bromus tectorum* L.
622 invasion in cold desert shrublands of western North America. *Ecosystems*. 17, 360-375.
623 <https://doi.org/10.1007/s10021-013-9725-5>.

624 Chambers, J.C., Maestas, J.D., Pyke, D.A., Boyd, C.S., Pellant, M., Wuenschel, A., 2017. Using Resilience
625 and Resistance Concepts to Manage Persistent Threats to Sagebrush Ecosystems and Greater Sage-
626 grouse. *Rangel Ecol Manag*. 70, 149-164. <https://doi.org/10.1016/j.rama.2016.08.005>.

627 Chambers, J.C., Roundy, B.A., Blank, R.R., Meyer, S.E., Whittaker, A., 2007. What makes Great Basin
628 sagebrush ecosystems invisable by *Bromus tectorum*? *Ecological Monographs*. 77, 117-145.
629 <https://doi.org/10.1890/05-1991>.

630 Chambers, J.C., Wisdom, M.J., 2009. Priority research and management issues for the imperiled Great
631 Basin of the western United States. *Restor Ecol*. 17, 707-714. [https://doi.org/10.1111/j.1526-
632 100X.2009.00588.x](https://doi.org/10.1111/j.1526-100X.2009.00588.x).

633 Davies, K.W., Bates, J.D., 2019. Longer-Term Evaluation of Sagebrush Restoration After Juniper Control
634 and Herbaceous Vegetation Trade-offs. *Rangeland Ecol Manag*. 72, 260-265.
635 [10.1016/j.rama.2018.10.006](https://doi.org/10.1016/j.rama.2018.10.006).

636 Davies, K.W., Bates, J.D., Boyd, C.S., 2018. Post-wildfire seeding to restore native vegetation and limit
637 exotic annuals: an evaluation in juniper-dominated sagerush steppe *Restoration Ecology*. 27, 120-127.
638 <https://doi.org/10.1111/rec.12848>.

639 Davis, M.A., Grime, P., Thompson, K., 2000. Fluctuating resources in plant communities: a general theory
640 of invasibility. *J Ecol*. 88, 528-534. DOI 10.1046/j.1365-2745.2000.00473.x.

641 Germino, M.J., Barnard, D.M., Davidson, B.E., Arkle, R.S., Pilliod, D.S., Fisk, M.R., Applestein, C., 2018.
642 Thresholds and hotspots for shrub restoration following a heterogeneous megafire. *Landsc Ecol*. 33,
643 1177-1194. <https://doi.org/10.1007/s10980-018-0662-8>.

644 Gu, Y., Wylie, B.K., 2010. Detecting ecosystem performance anomalies for land management in the
645 Upper Colorado River Basin using satellite observations, climate data, and ecosystem models. *Remote
646 Sens*. 2, 1880-1891. <https://doi.org/10.3390/rs2081880>.

647 Gu, Y.X., Wylie, B.K., Boyte, S.P., Picotte, J., Howard, D.M., Smith, K., Nelson, K.J., 2016. An Optimal
648 Sample Data Usage Strategy to Minimize Overfitting and Underfitting Effects in Regression Tree Models
649 Based on Remotely-Sensed Data. *Remote Sens*. 8, 943. <https://doi.org/10.3390/rs8110943>.

650 Herrick, J.E., Van Zee, J.W., McCord, S.E., Courtright, E.M., Karl, J.W., Burkett, L.M., 2017. Monitoring
651 Manual for Grassland, Shrubland, and Savanna Ecosystems. USDA - ARS Jornada Experimental Range:
652 Las Cruces, NM.

653 Jenkerson, C.B., Maiersperger, T.K., Schmidt, G.L., 2010. eMODIS—a user-friendly data source. U.S.
654 Geological Survey Open-File Report 2010-1055: Reston, VA.

655 Jensen, J.R., 2005. *Introductory digital image processing: A remote sensing perspective*. Pearson
656 Prentice Hall: Upper Saddle River, NJ. 526 p.

657 Monitoring Trends in Burn Severity. MTBS Data Access: Fire Level Geospatial Data.
658 <https://www.mtbs.gov/> accessed July 2018.
659 Pilliod, D.S., Welty, J.L., Arkle, R.S., 2017. Refining the cheatgrass-fire cycle in the Great Basin:
660 Precipitation timing and fine fuel composition predict wildfire trends. *Ecol Evol.* 7, 8126-8151.
661 <https://doi.org/10.1002/ece3.3414>.
662 PRISM Climate Group. Oregon State University. <http://prism.oregonstate.edu/> accessed 27 August 2015.
663 Quinlan, J.R. An Overview of Cubist. RuleQuest. <https://www.rulequest.com/> accessed 27 June 2019.
664 Quinlan, J.R. See5: An informal tutorial -- release 2.10. RuleQuest. <https://www.rulequest.com/>
665 accessed 27 June 2019.
666 Rau, B.M., Chambers, J.C., Pyke, D.A., Roundy, B.A., Schupp, E.W., Doescher, P., Caldwell, T.G., 2014. Soil
667 Resources Influence Vegetation and Response to Fire and Fire-Surrogate Treatments in Sagebrush-
668 Steppe Ecosystems. *Rangeland Ecol Manag.* 67, 506-521. <https://doi.org/10.2111/REM-D-14-00027.1>.
669 Rigge, M., Homer, C., Wylie, B., Gu, Y., Shi, H., Xian, G., Meyer, D.K., Bunde, B., 2019. Using remote
670 sensing to quantify ecosystem site potential community structure and deviation in the Great Basin,
671 United States. *Ecological Indicators.* 96, 516-531. <https://doi.org/10.1016/j.ecolind.2018.09.037>.
672 Rigge, M., Wylie, B.K., Gu, Y., Belnap, J., Phuyal, K., Tieszen, L.L., 2013. Monitoring the status of forests
673 and rangelands in the western United States using ecosystem performance anomalies. *Int J Remote*
674 *Sens.* 34, 4049-4068. <http://dx.doi.org/10.1080/01431161.2013.772311>.
675 Rose, R.A., Byler, D., Eastman, J.R., Fleishman, E., Geller, G., Goetz, S., Guild, L., Hamilton, H., Hansen,
676 M., Headley, R., Hewson, J., Horning, N., Kaplin, B.A., Laporte, N., Leidner, A., Leimgruber, P., Morissette,
677 J., Musinsky, J., Pintea, L., Prados, A., Radeloff, V.C., Rowen, M., Saatchi, S., Schill, S., Tabor, K., Turner,
678 W., Vodacek, A., Vogelmann, J., Wegmann, M., Wilkie, D., Wilson, C., 2015. Ten ways remote sensing
679 can contribute to conservation. *Conserv Biol.* 29, 350-359. <https://doi.org/10.1111/cobi.12397>.
680 Roundy, B.A., Chambers, J.C., Pyke, D.A., Miller, R.F., Tausch, R.J., Schupp, E.W., Rau, B., Gruell, T., 2018.
681 Resilience and resistance in sagebrush ecosystems are associated with seasonal soil temperature and
682 water availability. *Ecosphere.* 9, e02417. <https://doi.org/10.1002/ecs2.2417>.
683 Svejcar, T., Boyd, C., Davies, K., Hamerlynck, E., Svejcar, L., 2017. Challenges and limitations to native
684 species restoration in the Great Basin, USA. *Plant Ecol.* 218, 81-94. [https://doi.org/10.1007/s11258-016-](https://doi.org/10.1007/s11258-016-0648-z)
685 [0648-z](https://doi.org/10.1007/s11258-016-0648-z).
686 The National Land Cover Database. Department of Interior, U.S. Geological Survey.
687 <http://www.mrlc.gov/> accessed 28 June 2019.
688 U.S. Fish and Wildlife Service, 2013. Greater sage-grouse (*Centrocercus urophasianus*) conservation
689 objectives: Final report. U.S. Fish and Wildlife Service: Denver, CO.
690 Wylie, B.K., Boyte, S.P., Major, D.J., 2012. Ecosystem Performance Monitoring of Rangelands by
691 Integrating Modeling and Remote Sensing. *Rangeland Ecol Manag.* 65, 241-252.
692 <https://dx.doi.org/10.2111/Rem-D-11-00058.1>.
693 Wylie, B.K., Pastick, N.J., Picotte, J.J., Deering, C.A., 2018. Geospatial data mining for digital raster
694 mapping. *GIScience & Remote Sensing.* 56, 406-429. <https://doi.org/10.1080/15481603.2018.1517445>.
695 Wylie, B.K., Zhang, L., Bliss, N., Ji, L., Tieszen, L.L., Jolly, W.M., 2008. Integrating modelling and remote
696 sensing to identify ecosystem performance anomalies in the boreal forest, Yukon River Basin, Alaska. *Int*
697 *J Digit Earth.* 1, 196-220. <http://doi.org/10.1080/17538940802038366>.
698
699
700
701

702 **Table 1. Model accuracy assessments for the three datasets developed with regression-tree models. The relative**
 703 **error magnitude is the ratio of the average error magnitude to the error magnitude that would result from**
 704 **always predicting the mean value (Quinlan 2008).**

	<u>Training</u>			<u>Test</u>		
	Correlation coefficient (<i>r</i>)	Mean absolute error	Relative error	Correlation coefficient (<i>r</i>)	Mean absolute error	Relative error
Annual herbaceous	0.92	4.4	0.33	0.91	4.6	0.34
Sagebrush expected performance	0.97	1.7	0.20	0.97	1.7	0.20
Sagebrush site potential	0.98	1.1	0.16	0.98	1.1	0.17

705
 706
 707
 708
 709
 710
 711
 712
 713
 714
 715
 716
 717
 718
 719
 720
 721
 722
 723

724 **Table 2. Driving variables for the sagebrush condition class models. Frequency (%) of usage is shown for each**
 725 **variable for both models. Dashes indicate that a variable was not used. A 10-boost option was applied to the**
 726 **predictive model to improve model accuracy.**

Variable	% Variable usage	
	Predictive	Descriptive
Elevation	100	75
30-yr precipitation (ppt)	100	73
July temperature maximum (tmax)	100	14
Soil organic matter	100	4
March ppt	99	7
June temperature minimum (tmin)	95	6
July ppt	95	3
Available water capacity	94	18
March tmin	94	11
June ppt	93	4
July tmin	92	--
April ppt	90	6
March tmax	89	2
30-yr tmin	89	6
May ppt	88	--
August ppt	87	3
Spring ppt	87	--
April tmin	87	--
30-yr tmax	87	--
Summer ppt	85	--
April tmax	84	--
May tmax	79	--
August tmax	79	--
August tmin	77	--
Spring tmin	70	--
May tmin	69	--
June tmax	65	6
Spring tmax	57	--
Summer tmin	57	--
Summer tmax	27	--

The predictive model's training and test accuracies (*r*) equal 87.30% and 74.60%, respectively.
 The 10-fold cross validation accuracy (*r*) equals 73.70%.
 The descriptive model's training and test accuracies (*r*) equal 67.70% and 69.40%, respectively.

727
 728
 729

730 **Table 3. Weighted average by class and variable. These averages generally define the thresholds of the most**
 731 **influential variables within each class of the descriptive model.**

Class	Variable						
	Elevation (m)	30-y ppt (mm)	AWC	July tmax °C	March tmin °C	March ppt (mm)	Total area (%)
Recovery	1601.87	267.14	44.12	30.62	-2.74	26.26	21.29
Tipping point	1504.72	349.57	44.35	29.18	-2.8	28.49	70.36
Stable	1939.30	416.77	45.07	26.65	-5.38	40.49	8.35

732

733

734

735

736

737

738

739

740

741

742

743

744

745

746

747

748

749

750

751

752 **Table 4. Dominant variable thresholds by class gleaned from the descriptive model's rulesets. Threshold range is**
 753 **given, along with the ruleset(s) to which the threshold range applies. The weighted mean value for each**
 754 **dominant variable is reported for each class.**

Recovery class

dominant thresholds

Rulesets 1 - 7

Driver	Model threshold	Ruleset(s)	Ruleset(s) as % of total land area	Weighted class mean (μ)	Class range
Elevation (m)	>1451 to \leq 1602	2,3,4,6	4.53	1602	1442 - 1760
	>1339 to \leq 1602	1	7.16		
	>1602	7	9.11		
30-yr July tmax ($^{\circ}$ C)	>31	1,5	7.66	30.62	29.21 - 32.57
	\leq 30	2	<1		
	>30	4	1.46		
	>28 to \leq 31	6	<1		
30-yr March ppt (mm)	\leq 36	2,4,6	2.94	26.26	18.93 - 29.70
30-yr annual ppt (mm)	\leq 244	3	1.59	267.14	221.21 - 293.38
	\leq 338	7	9.11		

Tipping point class

dominant thresholds

Rulesets 8 - 16

Elevation (m)	>1602	9,12,15	2.51	1504.72	1169 - 1762
	\leq 1602	11,16	13.14		
	>1602 to \leq 1798	8	<1		
	\leq 1339	10	22.23		
30-yr annual ppt (mm)	\leq 338	9,12,13,	11.21	349.57	252.08 - 474.01
	>338	14	22.29		
March tmin ($^{\circ}$ C)	\leq -4	8	<1	-2.80	-4.27 - -1.09
	>-3	15	1.00		

Stable class

dominant thresholds

Rulesets 17 - 21

Elevation (m)	>1602	19,20,21	2.84	1939.30	1666 - 2129
	>2002	18	3.99		
	>1798	17	1.51		
30-yr annual ppt (mm)	≤338	17,19,20,21	4.35	416.77	264.50 - 562.94
	>338	18	3.99		
March tmin (°C)	≤-3	19,20,21	2.84	-5.38	-6.84 - -1.63

755 **Table 5. The Assessment Inventory and Monitoring (AIM) accuracy assessment by class and year for the**
756 **predictive sagebrush condition classes.**

Year	Class	Sample size	Number accurate	Percentage accurate
2013	Recovery	77	34	44.16
	Tipping point	234	152	64.96
	Stable	69	51	73.91
Sub total		380	237	62.37
2014	Recovery	76	27	35.53
	Tipping point	198	159	80.30
	Stable	47	34	72.34
Sub total		321	220	68.54
2015	Recovery	101	31	30.69
	Tipping point	227	189	83.26
	Stable	59	32	54.24
Sub total		387	252	65.12
2016	Recovery	153	62	40.52
	Tipping point	485	337	69.48
	Stable	126	79	62.70
Sub total		764	478	62.57
Total		1852	1187	64.09

774

775

776

777

778

779

780

781

782

783

784

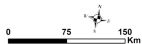
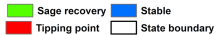
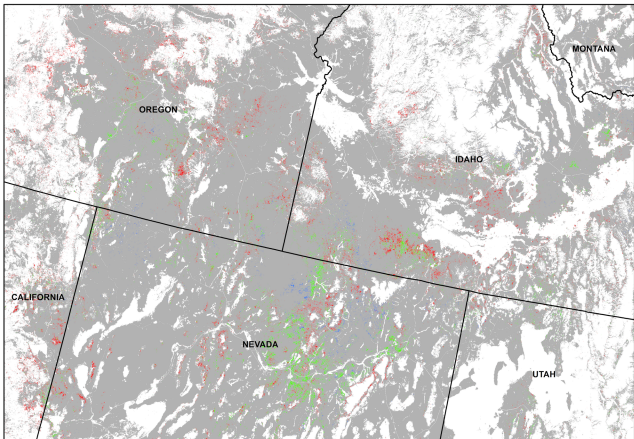
785 **Figure 1. Potential reference data points. Pixels that met the criteria from 4 datasets for one of 3 classes of**
786 **sagebrush condition are displayed. The mask (white inside map's borders) covers areas not classified as**
787 **herbaceous/grassland or shrubs by the 2011 National Land Cover Database (NLCD) and/or areas that are higher**
788 **than 2 250 m elevation.**

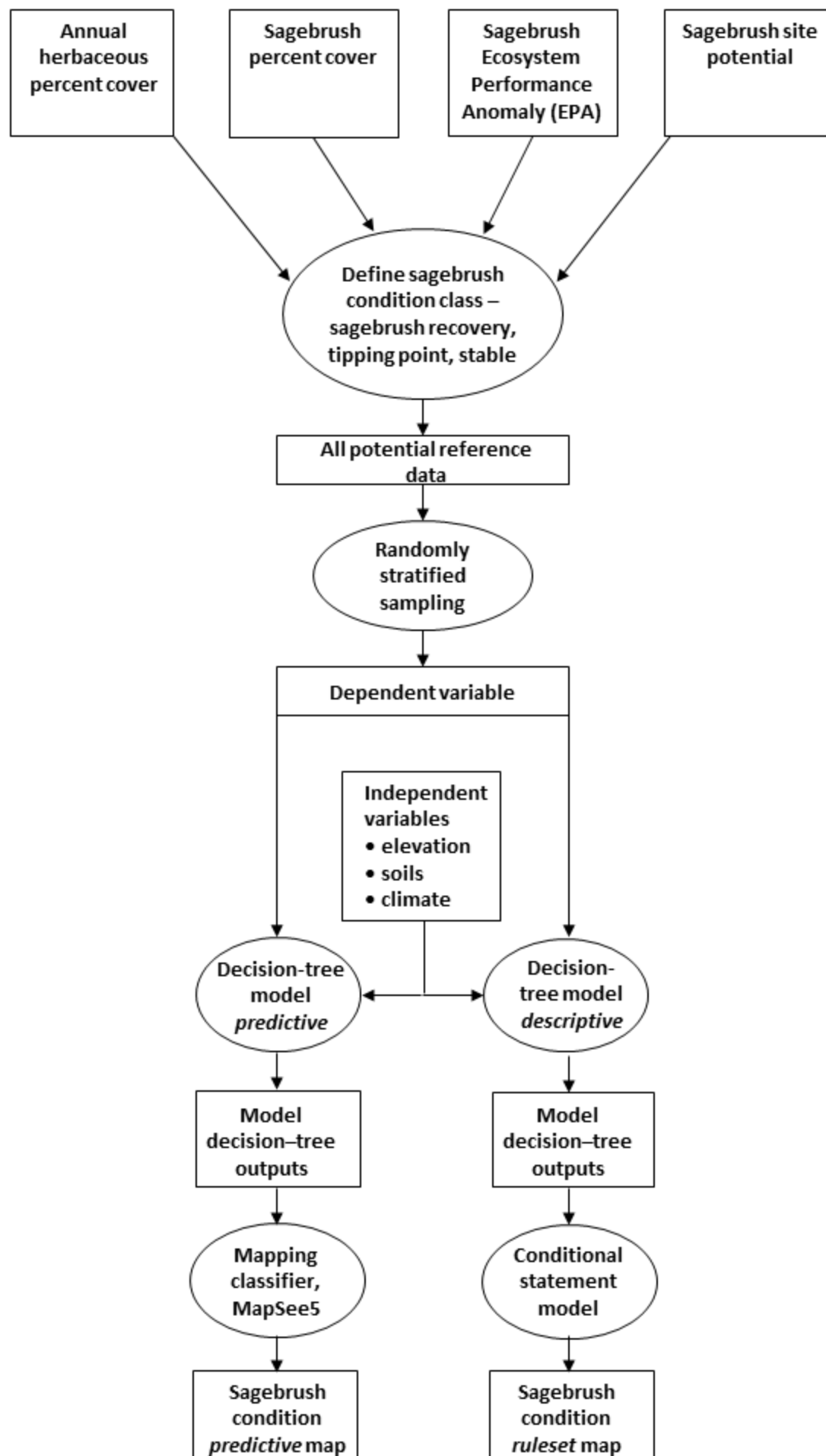
789 **Figure 2. Data and processes. The flowchart shows the data and outlines the processes used to develop the 2**
790 **sagebrush condition class maps. The data and processes are identical until the decision-tree modeling step**
791 **where we developed 1 model that used a tree-structure for predictive purposes and a second model that used**
792 **rulesets for descriptive purposes and the interpretation of abiotic thresholds of sagebrush condition class.**

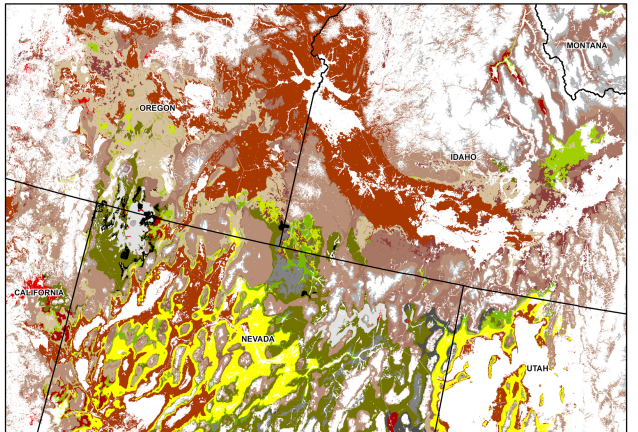
793 **Figure 3. A spatially explicit ruleset map. Each ruleset, or classifier, is defined by the variable(s) and its value(s)**
794 **used to establish if-then rules in the descriptive model. Rules 1 – 7 represent sagebrush recovery areas, 8 – 16**
795 **represent tipping point areas, and 17 – 21 represent stable areas. The rulesets are prioritized so that those with**
796 **higher accuracy spatially supersede those with lower accuracy when a pixel is defined by more than 1 ruleset.**
797 **The mask (white) covers areas not classified as herbaceous/grassland or shrubs by the 2011 National Land Cover**
798 **Database (NLCD) and/or areas that are higher than 2 250 m elevation.**

799 **Figure 4. A chart that displays each sagebrush condition class – sagebrush recovery, tipping point, or stable – as**
800 **a percent of the total area burned in the study area by year. We used a time dimension in our criteria to define**
801 **each class. This time dimension focused the transition from a degraded state to a sagebrush recovery class and**
802 **the transition from a stable sagebrush ecosystem state to a degraded state, or tipping point class, on the last 5**
803 **years of the time series. Given this time dimension, the last 5 years of the time series are most critical in**
804 **assessing the accuracy.**

805 **Figure 5. A spatially explicit predictive map. Each pixel is classified as one of 3 sagebrush condition classes and**
806 **delineated by confidence levels that ranged from 0.33 to 1.00 determined by a decision-tree model. A class**
807 **confidence level equal to or greater than 0.70 was labeled high probability; a class confidence level equal to or**
808 **greater than 0.50 and less than 0.70 was labeled moderate probability; and a class confidence level equal to or**
809 **greater than 0.33 and less than 0.50 was labeled low probability. The mask (white) covers areas not classified as**
810 **herbaceous/grassland or shrubs by the 2011 National Land Cover Database (NLCD) and/or areas that are higher**
811 **than 2 250 m elevation.**







Ruleset



0 100 200
Km



